Supplementary information

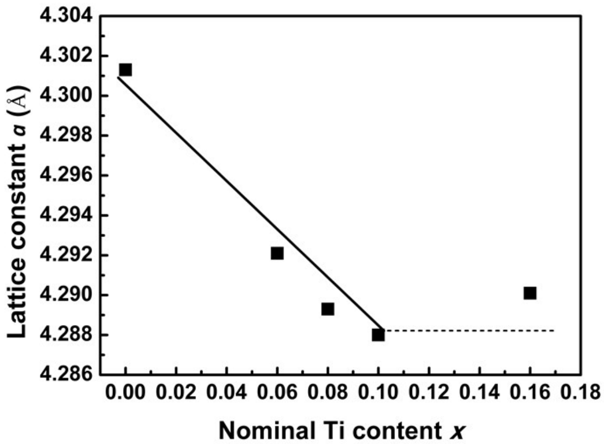

Fig. S1 Dependence of lattice constant on Ti content for $Ti_xBi_{0.5}Sb_{1.5-x}Te_3$ samples.

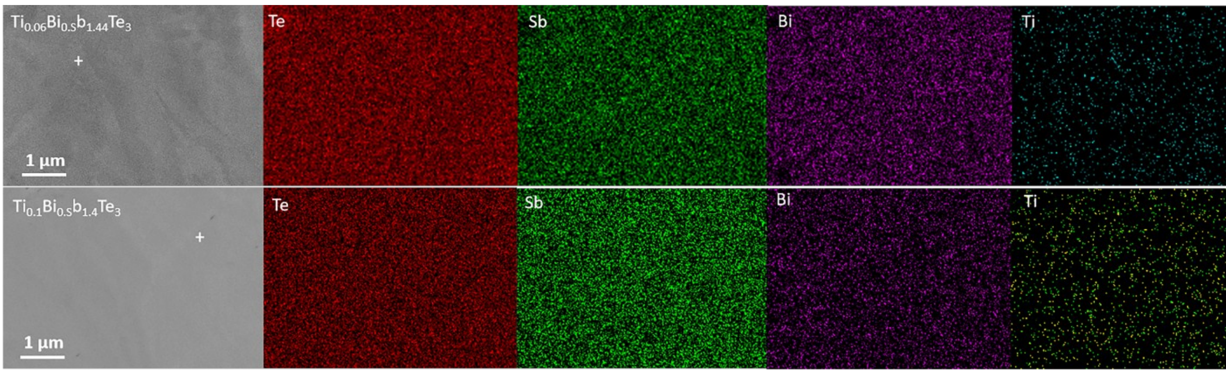

Fig. S2 Elemental mapping for the $Ti_{0.06}Bi_{0.5}Sb_{1.44}Te_3$ and $Ti_{0.1}Bi_{0.5}Sb_{1.4}Te_3$ samples.

Table S1. Measured composition of the $Ti_{0.06}Bi_{0.5}Sb_{1.44}Te_3$ and $Ti_{0.1}Bi_{0.5}Sb_{1.4}Te_3$ samples by EDS analysis.

Sample	Bi	Sb	Te	Ti	Measured composition
$Ti_{0.06}Bi_{0.5}Sb_{1.44}Te_3$	11.7	29.3	58.0	1.1	$Ti_{0.06}Bi_{0.61}Sb_{1.52}Te_3$
$Ti_{0.10}Bi_{0.5}Sb_{1.40}Te_3$	10.5	29.1	58.5	1.9	$Ti_{0.10}Bi_{0.54}Sb_{1.49}Te_3$

As shown in the Figure S2, the sample is a single phase without impurities and the Ti element presents in the matrix. Table S1 shows the measured composition of the sample by EDS analysis. Considering the accuracy of the EDS analysis, it is reasonable to conclude that the actual composition of our sample should be very close to its nominal composition.

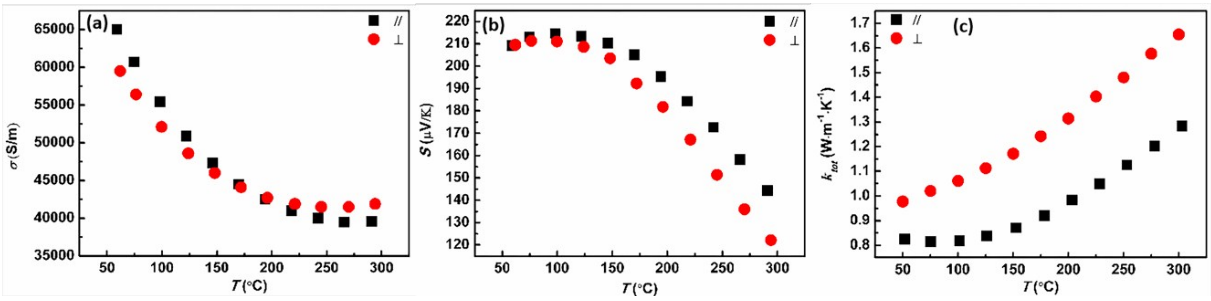

Fig. S3 Electrical and thermal properties of the $Ti_{0.06}Bi_{0.5}Sb_{1.44}Te_3$ in parallel/perpendicular hot pressure direction.

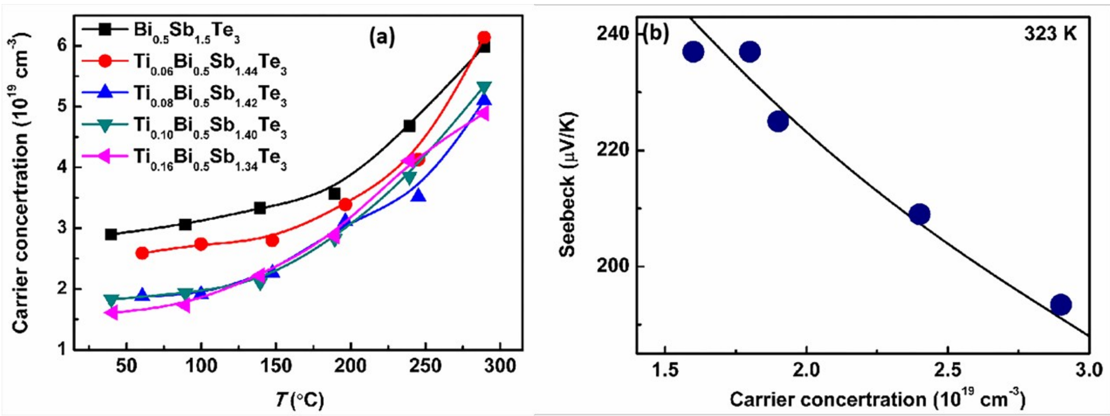

Fig. S4 (a) Temperature dependences of carrier concertration and (b)Pisarenko line for the $Ti_xBi_{0.5}Sb_{1.5-x}Te_3$ samples.

As shown in Fig. S4, the carrier concentration increases with both temperature and doped Ti concentration, and the doping of Ti has almost no effect on the band structure according to the Pisarenko line.

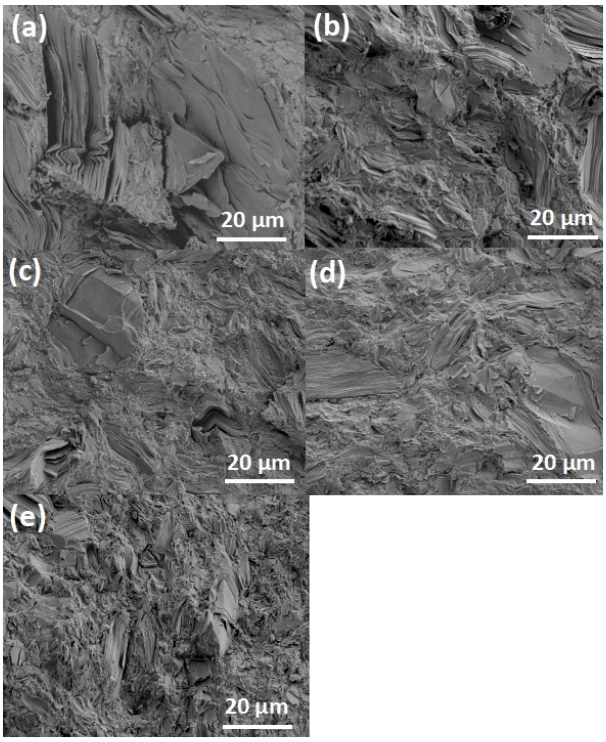

Fig. S5 SEM images of the fracture surfaces of the $Ti_xBi_{0.5}Sb_{1.5-x}Te_3$ samples for (a) x = 0, (b) x = 0.06, (c) x = 0.08, (d) x = 0.10, and (e) x = 0.16.

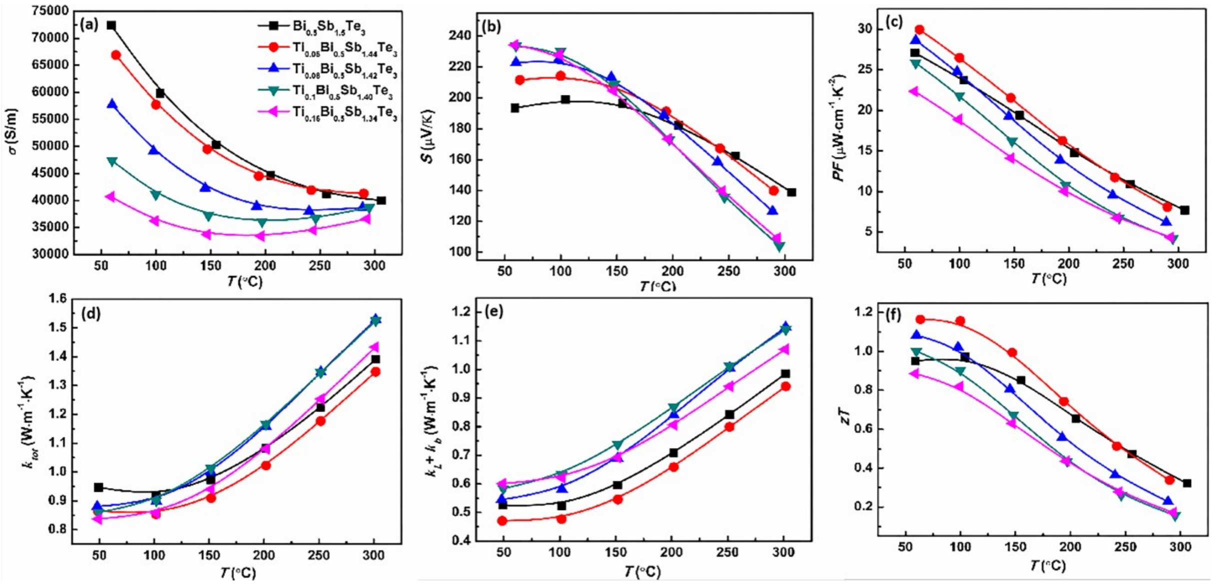

Fig. S6 Repeatedly measured data of the $Ti_xBi_{0.5}Sb_{1.5-x}Te_3$ samples.